2013

Brachyview: proof-of-principle of a novel in-body gamma camera for low dose-rate prostate brachytherapy

M Petasecca
University of Wollongong, marcop@uow.edu.au

K J. Loo
University of Wollongong, kjjl104@uowmail.edu.au

M Safavi-Naeini
University of Wollongong, mitra@uow.edu.au

Z Han
University of Wollongong, zh594@uowmail.edu.au

P E. Metcalfe
University of Wollongong, metcalfe@uow.edu.au

See next page for additional authors

Brachyview: proof-of-principle of a novel in-body gamma camera for low dose-rate prostate brachytherapy

Abstract

Purpose: The conformity of the achieved dose distribution to the treatment plan strongly correlates with the accuracy of seed implantation in a prostate brachytherapy treatment procedure. Incorrect seed placement leads to both short and long term complications, including urethral and rectal toxicity. The authors present BrachyView, a novel concept of a fast intraoperative treatment planning system, to provide real-time seed placement information based on in-body gamma camera data. BrachyView combines the high spatial resolution of a pixellated silicon detector (Medipix2) with the volumetric information acquired by a transrectal ultrasound (TRUS). The two systems will be embedded in the same probe so as to provide anatomically correct seed positions for intraoperative planning and postimplant dosimetry. Dosimetric calculations are based on the TG-43 method using the real position of the seeds. The purpose of this paper is to demonstrate the feasibility of BrachyView using the Medipix2 pixel detector and a pinhole collimator to reconstruct the real-time 3D position of low dose-rate brachytherapy seeds in a phantom. Methods: BrachyView incorporates three Medipix2 detectors coupled to a multipinhole collimator. Three-dimensionally triangulated seed positions from multiple planar images are used to determine the seed placement in a PMMA prostate phantom in real time. MATLAB codes were used to test the reconstruction method and to optimize the device geometry. Results: The results presented in this paper show a 3D position reconstruction accuracy of the seed in the range of 0.5-3 mm for a 10-60 mm seed-to-detector distance interval (Z direction), respectively. The BrachyView system also demonstrates a spatial resolution of 0.25 mm in the XY plane for sources at 10 mm distance from Medipix2 detector plane, comparable to the theoretical value calculated for an equivalent gamma camera arrangement. The authors successfully demonstrated the capability of BrachyView for real-time imaging (using a 3 s data acquisition time) of different brachytherapy seed configurations (with an activity of 0.05 U) throughout a 60 × 60 × 60 mm3 Perspex prostate phantom. Conclusions: The newly developed miniature gamma camera component of BrachyView, with its high spatial resolution and real time capability, allows accurate 3D localization of seeds in a prostate phantom. Combination of the gamma camera with TRUS in a single probe will complete the BrachyView system. © 2013 American Association of Physicists in Medicine.

Keywords

dose, low, camera, gamma, prostate, body, rate, novel, principle, proof, brachyview, brachytherapy

Disciplines

Engineering | Science and Technology Studies

Publication Details

Petasecca, M., Loo, K. J., Safavi-Naeini, M., Han, Z., Metcalfe, P. E., Meikle, S., Pospisil, S., Jakubek, J., Bucci, J., Zaider, M., Lerch, M. L. F., Qi, Y. & Rosenfeld, A. B. (2013). BrachyView: Proof-of-principle of a novel in-body gamma camera for low dose-rate prostate brachytherapy. Medical Physics, 40 (4), 041709-1-041709-9.

Authors

M Petasecca, K J. Loo, M Safavi-Naeini, Z Han, P E. Metcalfe, S Meikle, S Pospisil, J Jakubek, Joseph Bucci, Marco Zaider, M L. F Lerch, Y Qi, and Anatoly B. Rosenfeld

Brachy*View*: Proof-of-principle of a novel in-body gamma camera for low dose-rate prostate brachytherapy

M. Petasecca [a)], K.J. Loo [a)], M. Safavi-Naeini [a)], Z. Han [a)], P.E. Metcalfe [a)], S. Meikle [e),a)], S. Pospisil [d)], J. Jakubek [d)], J.A. Bucci [c)], M. Zaider [b)], M.L.F. Lerch [a)], Y. Qi [a)] and A.B. Rosenfeld [a)]

[a)] Centre for Medical Radiation Physics, University of Wollongong, Wollongong, NSW 2522, Australia

[b)] Dept. of Medical Physics, Memorial Sloan-Kettering Cancer Center, New York, NY 10021, USA

[c)] St George Cancer Care Centre, St George Hospital, Kogarah NSW 2217, Australia

[d)] Institute of Experimental and Applied Physics, Czech Technical University of Prague, Prague, Czech Republic

[e)] Brain and Mind Research Institute, University of Sydney, NSW 2006, Australia

Abstract

***Purpose*:** The conformity of the achieved dose distribution to the treatment plan strongly correlates with the accuracy of seed implantation in a prostate brachytherapy treatment procedure. Incorrect seed placement leads to both short and long term complications, including urethral and rectal toxicity. We present Brachy*View,* a novel concept of a fast intra-operative treatment planning system (ITPS), to provide real-time seed placement information based on in-body gamma camera data. Brachy*View* combines the high spatial resolution of a pixellated silicon detector (Medipix2) with the volumetric information acquired by a trans-rectal ultrasound (TRUS). The two systems will be embedded in the same probe so as to provide anatomically correct seed positions for intra-operative planning and post-implant dosimetry. Dosimetric calculations are based on the TG-43 method using the real position of the seeds. The purpose of this paper is to demonstrate the feasibility of Brachy*View* using the Medipix2 pixel detector and a pin-hole collimator to reconstruct the real-time 3D position of low dose rate brachytherapy seeds in a phantom.

Method: Brachy*View* incorporates three Medipix2 detectors coupled to a multi-pinhole collimator. Three-dimensionally triangulated seed positions from multiple planar images are used to determine the seed placement in a PMMA prostate phantom in real time. MATLAB codes were used to test the reconstruction method and to optimise the device geometry.

Results: The results presented in this paper show a 3D position reconstruction accuracy of the seed in the range of 0.5 mm and 3 mm for a 10 mm to 60 mm seed-to-detector distance interval (*Z* direction), respectively. The Brachy*View* system also demonstrates a spatial resolution of 0.25 mm in the *XY* plane for sources at 10 mm distance from Medipix2 detector plane, comparable to the theoretical value calculated for an equivalent gamma camera arrangement. We successfully demonstrated the capability of Brachy*View* for real-time imaging (using a 3 seconds data acquisition time) of different brachytherapy seed configurations (with an activity of 0.05 U) throughout a 60x60x60 mm^3 Perspex prostate phantom.

Conclusion: The newly developed miniature gamma camera component of Brachy*View*, with its high spatial resolution and real time capability, allows accurate 3D localization of seeds in a prostate phantom. Combination of the gamma camera with TRUS in a single probe will complete the Brachy*View* system.

Keywords— **Intra-operative planning system, Brachytherapy, 3D seed position reconstruction, QA, Brachy*View***

I. INTRODUCTION

Prostate cancer is one of the most commonly diagnosed cancers in the Western World, accounting for approximately 30% of all male malignancies [1]. Historically, the preferred treatment choice for localized prostate cancer has been radical prostatectomy [2]. More recently, there has been an increasing shift towards radiation treatment, with brachytherapy at the forefront of treatment options. When treated with brachytherapy, freedom from biochemical relapse is in the range of 75%-100% at 5 years and 66%-88% at 8-13 years [3]. However, in terms of distant failure and cause-specific survival all modalities appear to perform equally well.

Permanent prostate brachytherapy (PPB) implants are currently performed with ^{125}I or ^{103}Pd sources using ultrasound guidance to deliver high doses of localised radiation to the prostate gland [4]. The effectiveness of PPB is due to its ability to deliver a relatively high dose in a very conformal fashion to the target. Several reports in the literature[5][6][7][8] indicate the target coverage with 100% of the prescription doses is often less than 90% and the dose to normal tissues such as the urethra and rectum are highly variable. While an experienced physician can lessen the magnitude of these differences, many factors controlling execution of the plan are subject to random fluctuation. In low dose rate (LDR) brachytherapy, ^{125}I seeds are inserted transperineally via implant needles into the prostate gland. Constraints on the critical structure dose (e.g. rectum, urethra) are set in the treatment planning system (TPS).

In PPB, post implant dosimetry studies[8] on patients show that accurate pre-planning correlates with good (86% and 89%) target volume coverage with prescription dose (V_{100} and V_{90}, respectively); the agreement to prescription dose increases to over 96% (V_{100}) and 98% (V_{90}) of target volume when the plan is modified and re-calculated intra-operatively taking into account the real needles positions in contrast to positions assumed by template (intraoperative conformal optimization and planning named I-3D). Intraoperative planning is achieved by using trans-rectal ultrasound (TRUS) as the standard imaging modality for volumetric prostate studies and accurate needle position determination in a prostate gland.

An alternative technique developed by Wallner et al. [9], uses computed tomography (CT) to identify the position and shape of the prostate for treatment planning; however, the ability to “see” the prostate in a CT study is known to be rather poor. In this technique, intraoperative needle placement is verified under fluoroscopy using the urethra as the primary reference marker.

The use of CT-guided insertion of the needles has also been investigated in the recent past [10][11] but its widespread use is limited by high cost. Recently Zelefsky et al. [12] demonstrated, using cone beam CT (O-arm), a technique for seed placement verification and its comparison with the TPS; the system is equipped with software fully developed at Memorial-Sloan-Kettering Cancer Center (MSKCC) - New York for fusion of the CT-imaged seeds with planned seeds in a prostate. This

system was used in the operating room after all seeds were implanted rather than during the procedure to avoid undesirable time delay. This procedure allows the implantation of additional seeds in cold spots thus identified.

The traditional preplanned approach used for PPB has limitations that may be overcome by intraoperative dynamic treatment planning (IDTP). MSKCC has developed and successfully implemented I-3D for ultrasound (TRUS) based ITP, obviating the need for pre-planning [13]. However IDTP requires knowledge of location of each dropped seed in a prostate follow by fast re-planning. While a TRUS-based ITP system is a suitable method for prostate volumetric studies and needle guidance, some physicians remain skeptical of its seed position identification accuracy [14][15][16].

Seed location determination is crucial for verification of the planned treatment to minimize toxicity to the surrounding organs and IDTP plays an important role in compensation for seeds misplacement to keep dosimetry optimal. While contemporary radiotherapy technology is quite precise there remains questions on the possibility of reliable real time quality check (QC) to avoid possible accidents reported previously [17][18].

The above discussion indicates that real-time QC is imperative to maximise the benefits of PPB while keeping the dose constraints to critical organs in check. This paper discusses the proof–of–concept of a novel in-body imaging technique using a high spatial resolution gamma camera embedded in a TRUS probe for real-time in-vivo seed identification concurrent with a prostate ultrasound image dataset. The QC system, called Brachy*View* was designed to provide this information.

II. MATERIAL AND METHODS

A. Brachy*View* rectal probe

The Brachy*View* rectal probe design is based on a multi-pinhole lead collimator and three side-by-side Medipix2 detectors[19][20] with a total imaging area of 14x42 mm^2 (256x768 pixels with individual pixel size of 55x55 μm^2) and was manufactured in collaboration with the Institute of Experimental and Applied Physics of the Czech Technical University of Prague. The radioactive seeds are the source of the imaging radiation and are projected through the pinholes onto the detector surface (Fig. 1). In contrast to a traditional pinhole gamma camera this system works in demagnification mode (magnification factor less than 1), an attribute made possible by the unique spatial resolution of the Medipix2 detector. In Medipix2, each pixel has an independent pre-amplification channel and two discriminator levels. Therefore when a photon is detected by a pixel and its energy deposition generates a signal larger than the threshold, the corresponding counter increases by one count and is digitally readout by a USB interface with a refresh rate of a few hundred Hz[20]. The count map realizes a projection of the seed on the imager plane. Using a few distinct projections of the same seed through different pinholes, 3D seed

coordinates in the coordinate frame related to the TRUS system (mounted into the same probe) can be obtained using triangulation.

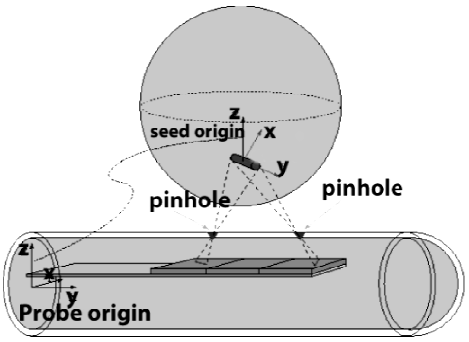

Fig. 1: Schematic of Brachy*View* rectal probe. Three side –by –side Medipix detectors are placed inside of the TRUS probe and inferiorly to the prostate gland.

B. Pinhole collimator design

The pinhole collimator used for feasibility studies has been developed at the Centre for Medical Radiation Physics (CMRP) and consists of a cone shaped lead structure (Fig.2a). A scanning electron microscope picture of the pinhole aperture used during the experiments is shown in Fig.2b. The combination of one Medipix2 detector and the collimator was designed to have a minimum Field Of View ($FOV \approx 2\ l\ \tan(\theta)$; l is the source-to-collimator distance)[21] of approximately 50 mm at a distance of 10 mm. The angle θ formed by the aperture (with the shape of a truncated cone with large face diameter D, small face diameter d and thickness T in Fig.2a) is $\pm 50.5°$, and was established based on the minimum distance between inner rectal wall (where the surface of the collimator/probe is to be placed) and prostate which is approximately 10 mm[22].

The thickness of the lead plate (T) is approximately 400 µm to attenuate the 22 – 35 keV photons emitted by the ^{125}I seeds. The aperture d was calculated to maximise the Medipix2 detector count rate (N, proportional to d^2) for fast real time seed identification without compromising the gamma camera spatial resolution (inversely proportional to d) for accurate seed position determination.

Using the model of Fig.2a, the count rate N can be estimated by considering the product of the portion of solid angle of a point source with activity A (decays/s) at distance R from the detector surface. The seed has been represented by a point source, identified in the the centre-of-mass of the seed, because the aim of this study is the evaluation of the performance of Brachy*View* for the reconstruction of the seed position regardless of its orientation.

— where —, r is the radius of the projected area through the pinhole, is the total efficiency due to Compton and photoelectric effects in silicon for 27 keV gamma photons (approximately 0.6 in a 400 µm thick silicon detector).

Considering a typical brachytherapy source air KERMA strength of 0.5 U that corresponds to intrinsic activity of 0.4 mCi[23] it is found that for an aperture of *d*=180 μm the expected count rate of the gamma camera exposed to a seed located at source-to-collimator distance of 50 mm would be approximately N=2700 counts/s. The above calculation shows that the geometry and dimensions of the system makes the use of the gamma camera for fast seed positioning determination possible, especially when only a few hundred counts are sufficient to discriminate the seed projection from the background noise.

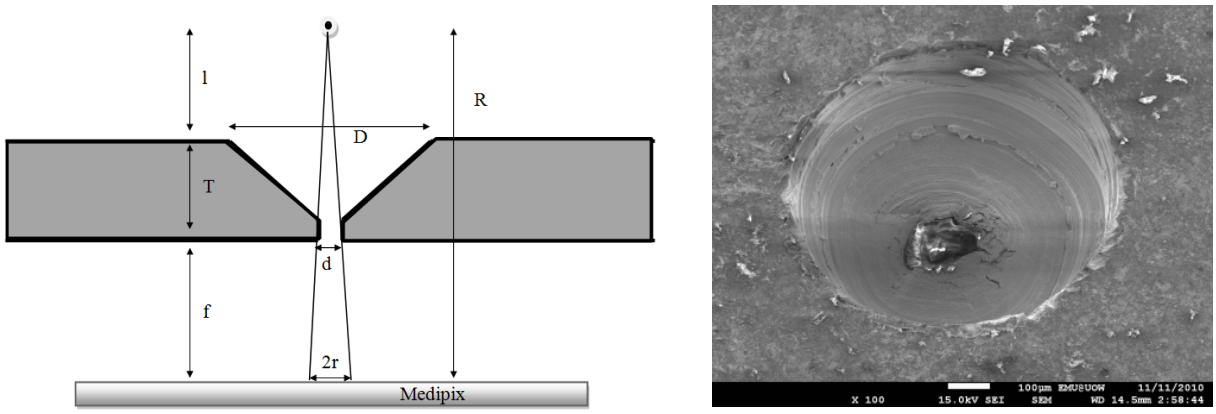

a) b)

Fig.2: a) Model of the pinhole used for the design of the collimator/camera setting; b)Scanning Electron Microscope of the pinhole for evaluation of the real dimensions of the aperture used during the experiments.

Experimentally, the seed position reconstruction technique was tested using a 60x60x60 mm^3 PMMA prostate phantom. Parallel channels for housing of the ^{125}I seeds were drilled horizontally following the standard grid template for the LDR TRUS-guided brachytherapy (Fig. 3). In this proof-of-concept study, a single Medipix2 with imaging plane 14x14 mm^2 and a single pin-hole lead collimator was used. The phantom was translated relative to the pinhole/detector system in order to achieve multiple images of the same seed. In addition, five pinhole collimators above the imaging detector were modeled using five separate projections.

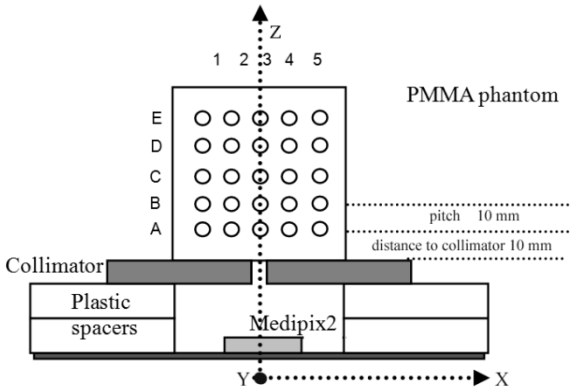

Fig.3: Schematic of the prostate phantom setup for seed image acquisition based on a single Medipix. The pitch of the holes housing the seeds is 10 mm. The distance between the sensor surface and the collimator 5.5 mm and the minimum distance of a seed from the collimator is approximately 10 mm. The prostate phantom is a block of PMMA of 60x60x60 mm^3

For the accurate translation of the phantom above the pinhole/detector, a motorised linear stage with bidirectional accuracy of ±10 μm in both X and Y directions was used.

C. 3D reconstruction method

The three-dimensional position of each seed is reconstructed by using a stereoscopic back-projection technique based on tracing lines between the pinholes and the centre of mass of the digitised 2D images of each seed on the plane of the Medipix2 detector. The positioning of the detector inside the rectum has two major consequences in terms of image reconstruction: a) it doesn't allow a rotation of the detector around the target region therefore a standard image reconstruction technique such as the multiple back-projection used in SPECT scanner cannot be adopted, b) due to space restrictions the pinhole camera has a magnification factor smaller than one, therefore an imaging sensor with a high spatial resolution is necessary.

The back-projection reconstruction method to be used with the Brachy*View* probe is based on the use of 2D images generated by the incident gamma rays from the seed projected onto the sensor plane through the pinhole collimator. The pinhole is identified as the origin of the camera frame (X_{c0}, Y_{c0}).

The image is the projection of a 3D object onto the detector plane assuming that each point of the object emits a gamma photon. To a first approximation, the image of the object can be represented by its centre of mass ignoring, at this stage, any information about its orientation. By acquiring at least two images of the object through two different positions of the collimator it is possible to reconstruct the position of the object in space from the intersection of the two lines calculated using the coordinates of the centre of mass of the images and the pinhole.

The system 'object-pinhole-2D projection' can be represented by a simple model that describes the mathematical relationship between the coordinates of the "3D point" P_c in the pinhole camera frame (X_c,Y_c,Z_c) and its projection P_1 onto the image plane (x,y) (Fig. 4). This model is based on the use of an ideal camera without lenses and thus without spherical distortion[25]. Equation (1) expresses the relationship between (X_c,Y_c,Z_c) and (x,y) by the focal length f_x=f_y=f assuming no astigmatic aberration in the system (square pixel size, square pixel array, cylindrical symmetry of the pinhole):

$$x = f\frac{X_c}{Z_c}; y = f\frac{Y_c}{Z_c} \quad (1)$$

If the origin of the image coordinate system is not in the centre of the image plane, the displacement (s_1,s_2) from the origin to the centre of the image plane is included in the projection equations, obtaining the perspective projection equation (2). The parameter s_i could represent any movement of the point P_c relative to the pinhole.

$$x = f\frac{X_c}{Z_c} + s_1; y = f\frac{Y_c}{Z_c} + s_2; \mathrm{z} = \mathrm{Z_c} \qquad (2)$$

The previous relation can be reformulated using the projective geometry framework, as

$$(\alpha x, \alpha y, \alpha)^T = (fX_c + s_1, fY_c + s_2, Z_c)^T \rightarrow \overline{P_1} = H\overline{P_c} \qquad (3)$$

where $\alpha=Z_c$ is the homogeneous scaling factor, H is the intrinsic conversion matrix composed by the parameters which characterise the pinhole-imager apparatus in the camera frame.

The above model was implemented in MATLAB and intrinsic parameters have been set with the values used for the experimental setup and reported in Tab.1.

Table 1: Intrinsic parameters of the homogeneous coordinate model as implemented in MATLAB.

Parameter	Symbol	Value
Focal length	$f=f_x=f_y$	5.5 ± 0.1 mm
Relative *X* translation P-to-pinhole	s_1	0
Relative *Y* translation P-to-pinhole	s_2	Steps of ±5 ± 0.01 mm
2D projection image centre-of-mass	*(x,y)*	Calculated by a Gaussian fit of the pixel map

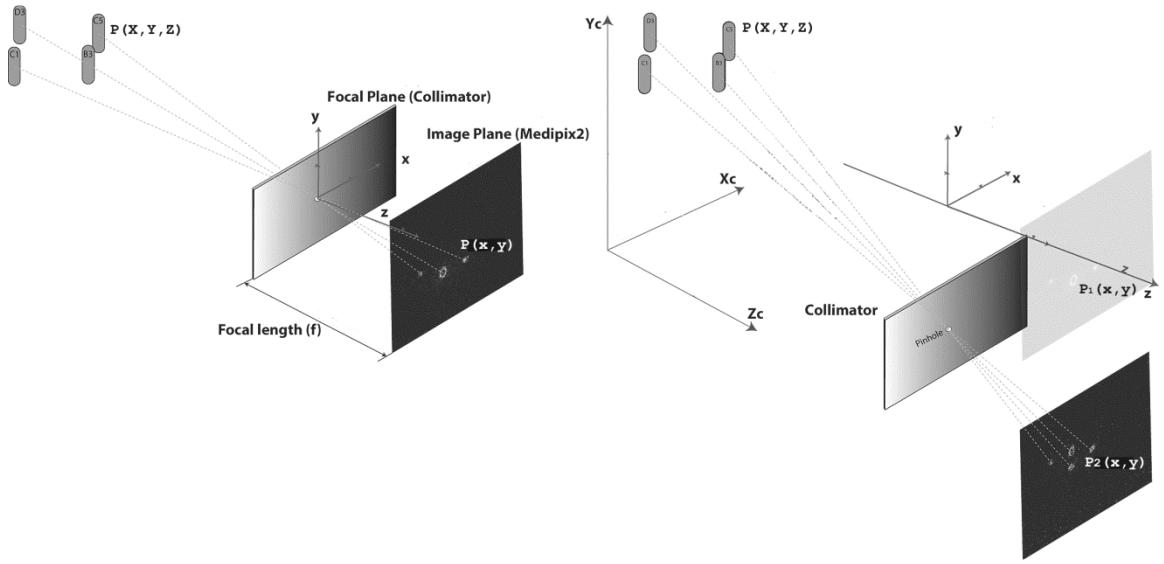

Fig.4: Schematic representation of the homogeneous coordinate model and reconstruction method by triangulation. The left side figure represents the first projection of the seeds: seed D3 is blocked by seed B3 and in the image plane only three seeds are visible. In the right side figure, the grey image plane represents the first projection; after a translation step backward to *Y* direction of the probe, all 4 seeds are visible on the image plane.

Using MATLAB algorithms in a three-dimensional geometry, rays are drawn from the projected seed image on the image plane (centre-of-mass of the projection) through the centre of the pinhole. This process is repeated every time the pinhole/detector is moved relative to the source. Since skew lines in 3D do not necessarily intersect, the seed coordinate P_c is assumed to be the midpoint of the shortest chord joining the two projected rays.

III. EXPERIMENTAL RESULTS

A configuration of 4 seeds (Model 6711 ^{125}I Oncura/GE Healthcare, Princeton, USA) with strength 0.05 U, were placed in positions B1, C2, B3, A4 of the phantom (Fig.3). Data that was acquired for three seconds at 50 frames/s, was used to evaluate the spatial resolution of Brachy*View* and estimate the effective diameter of the pinhole collimator. The seeds were positioned in three different rows to (i) evaluate the effect of the source-to-collimator distance (SCD), (ii) evaluate the projected image quality of two seeds positioned simultaneously: one in B3 (close to the detector and hence bright) and one in C2 (afar from the detector and hence weak); (iii) verify the extension of the FOV when a seed was placed in the periphery position (A4). The spatial resolution and pinhole effective diameter (d_{eff}) were evaluated assuming a Gaussian fit of the projections of the seeds onto the Medipix2 detector image plane. Due to the alignment of the detector relative to the phantom the numerals in Y direction corresponds to the column number of Medipix2 which are perpendicular to the long axis of the seeds. In this case the seeds appear horizontal on the image generated by the detector. Fig.5a shows the response map (image plane) of the system with four seeds in position. The response function can be represented in a plot by selecting one of the pixel columns (perpendicular to *X* direction), i.e. in Fig. 5b *Y*=120 (total number of columns is 256) was selected. The intensity distribution of the counts in the pixels along the *X* direction can be then used to calculate the spatial resolution and taking the imager pixel size and focal length into account, the effective diameter of the pinhole can be obtained.

The precision of 3D position reconstruction can be defined by the combination of the transverse and the longitudinal accuracy. Transverse accuracy ε_{xy} is the degree of closeness of the reconstructed position of the seed to the expected value in the *XY* plane (parallel plane to the collimator plane) and obtained by the back projection of the image through the pinhole. This quantity is related to the spatial resolution achievable in the plane of the imager (R_p) and it depends also on the dimension of the pinhole d_{eff} in the pinhole camera resolution R_t [24]. The spatial resolution R_p as a function of the SCD and the overall transverse accuracy ε_{xy} are plotted in Fig.5c (dash line and solid line, respectively). ε_{xy} matches the experimental data for a value of the effective diameter of the pinhole (d_{eff}) equal to 350 μm.

$$\varepsilon_{xy} = \sqrt{R_p^2 + R_t^2} = \sqrt{\left[\left(\frac{l}{f}\right)p\right]^2 + \left(\frac{d_{eff}(l+f)}{f}\right)^2} \qquad (4)$$

Equation (4) is entirely defined by the camera parameters: p is the detector pixel size, l is the SCD, d_{eff} is the effective pinhole diameter and f the focal length. The result obtained by Beekman is confirmed also by the work of Marks and Brady [24] based on 3D Fourier transformation of intensity maps of the source projected by a pinhole collimator. The comparison of the transverse accuracy calculated by (4) and measured by Brachy*View* is plotted in Fig. 5c.

The model developed by Marks and Brady allows also the calculation of the longitudinal accuracy (along Z direction) based only on the fundamental camera parameters:

$$\varepsilon_z \approx \frac{l^3 \cdot d}{f^2 \cdot s_2} \qquad (5)$$

where s_2 is the increment used for translation of the camera relative to the source (Tab.1). The longitudinal accuracy of Brachy*View* calculated by this model is ranging from ±0.2 mm at 10 mm SCD up to ±6 mm at 60 mm SCD (corresponding to the superior and anterior sides of prostate gland).

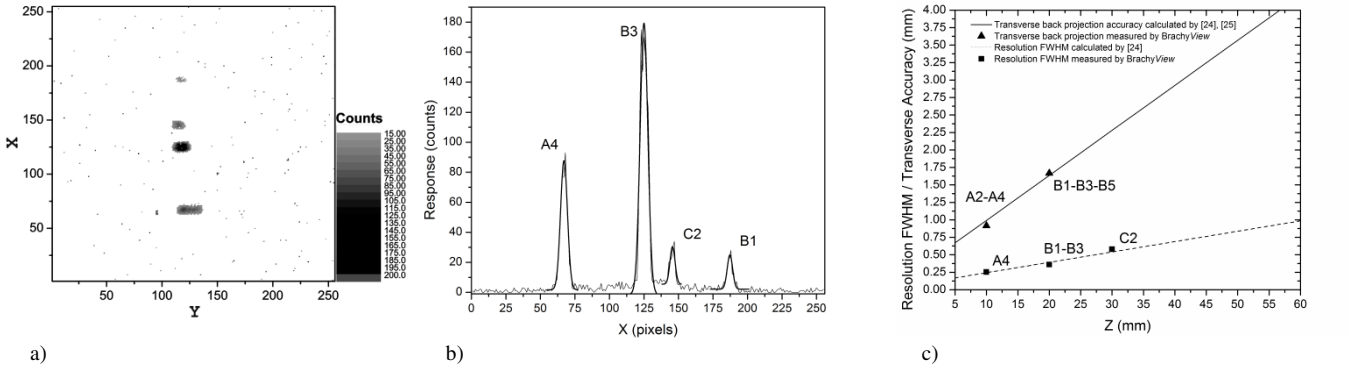

Fig.5: a) Response map of Brachy*View* to 4 seeds placed into positions B1, C2, B3, A4 of the phantom; b) response profile at column Y=120 and fit by Gaussian distribution for calculation of the spatial resolution FWHM; c) comparison of FWHM values obtained from the response map of the Brachy*View* camera (solid squares) and transverse accuracy in the plane XY (solid triangles) for different Z positions of seeds and predicted by the model from Beekman[23][25] and from Marks[24].

The 3D position reconstruction algorithm was tested by identifying five seeds placed in different positions of the XZ plane within the phantom, yet the same Y value. The position of the seeds was chosen to test two parameters that potentially affect the reconstruction technique: a) the blurring of the image and increasing of the background counts generated by scattered and penetrating photons through the lead, which is particularly significant when the seeds are in close proximity to the collimator (seeds located in the row A and B), and b) the evaluation of the image generated by masked seeds (i.e. the configuration with one seed in B1 and one in A2 is of interest because B1 is masked by A2 in the third projection of Fig. 6a). Reconstruction was carried out by the use of five projections (Fig. 6a) corresponding to a shift of the phantom in the Y direction to -10, -5, 0, 5 and 10 mm from the origin, respectively. The first image is taken with the centre of the detector aligned with the phantom in the position Y=-10 mm. Each successive image of the sequence is taken after a 5 mm incremental shift of the detector-

pinhole toward positive *Y* (Fig. 6b). This technique aims to mimic the use of a multiple pinhole collimator and a detector surface equivalent to a triple Medipix2 configuration as planned for the final prototype.

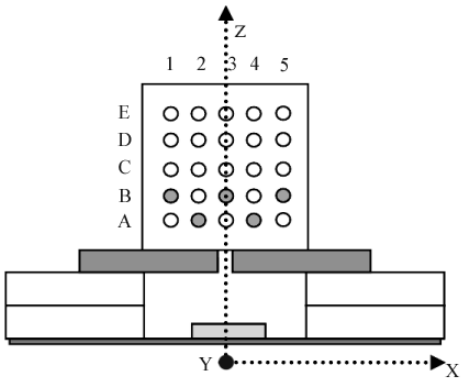

a) b)

Fig.6. a) Medipix response maps of 5 implanted seeds at positions A2, A4, B1, B3, B5. The shape of each seed is clearly visible. Note that in the third image at the top, the seeds in positions B1 and B5 are blocked from view by seeds in row A. Each view is taken at 5mm increments along the *Y*-axis. b) schematic representation of the seeds inside the phantom.

Accuracy of the 3D coordinate reconstruction decreases with SCD, however the center of the seeds placed at row E corresponding to 60 mm SCD can still be fully resolved and localized with an accuracy of 3 mm (Fig. 7).

Fig.7: Medipix response map of 5 seeds implanted at positions E1, E2, E3, E4 and E5. The shape of each seed is not visible anymore but the centre of mass can be still resolved and used for 3D reconstruction of the seed position.

IV. DISCUSSION

The above results show that 3D reconstruction of ^{125}I seeds using a pinhole camera inserted into the rectum is feasible with some limitations given by the specific setup used in these experiments. The main parameters characterized in this work are the transverse and longitudinal resolution of the camera. The transverse spatial resolution measured at low SCD is in the sub-millimeter range and matches the requirements for accurate localization of the source. On the other hand, for a 60 mm

SCD the resolution is approximately ±4 mm which seems to be inadequate for accurate position reconstruction of the seeds. This limitation can be addressed by the employment of a tungsten pinhole collimator manufactured by laser etching techniques[25] which will reduce the effective pinhole diameter down to 150-180 µm. The estimation of the count rate N will still be acceptable with 2700 counts/s but the transverse resolution will be substantially improved (2 mm transverse resolution at SCD of 60 mm, accordingly with the Marks and Brady model described above).

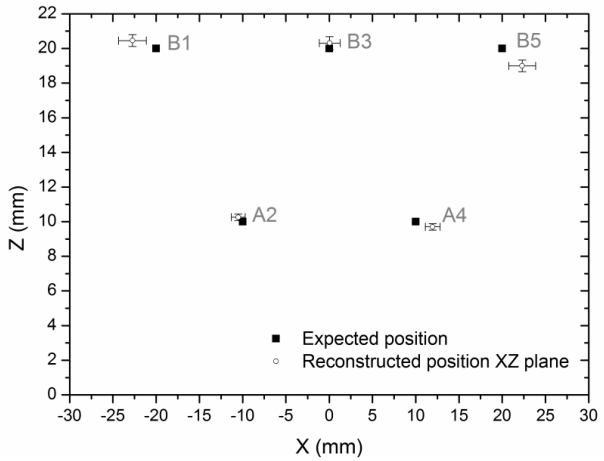

Fig.8: Comparison of the reconstructed and expected seed positions in a phantom based on the centre-of-mass of the seeds in the *XZ* plane; *Y* is kept constant.

The longitudinal resolution is, by comparison, very robust. It is affected only by the focal length ($\propto 1/f^2$) which therefore must be determined very accurately. Data in Fig.8 shows that the effect of an uncertainty of ±100 µm on the focal length generates a variation (vertical error bars) of the seed reconstructed position in Z of less than 1 mm.

The horizontal error bars are calculated by the model for the transverse accuracy of equation (4). The model predicts the uncertainty obtained in the experimental data and confirms the importance of accurate manufacturing of the pinhole collimator to optimize the 3D reconstruction accuracy. All the parameters have been investigated considering a linear source embedded in the titanium shell and its projection is simplified by the identification of the centre of mass of the seed image. This approach should still be valid for brachytherapy seeds with radioactive material embedded in small beads encapsulated into titanium shell. Photon scattering in the Ti shell of the seed will smooth the effect of the discrete distribution of the radioactive material inside the seed especially at high SCD and the approximation of the seed projection profile by a Gaussian fit should still be possible. The main advantage of this technique we would like to highlight in this work is the possibility to co-register the 3D dataset obtained by the pinhole camera with the images of the prostate obtained by the TRUS probe. The overall dimensions of the camera are small enough to be integrated in a 22 – 24 mm diameter cylindrical probe which still represents an acceptable size for use with patients [26]. Although the integration of the two devices in a single instrument is challenging from an engineering point of view, the co-registration of the datasets will be simple. The instrument will have

the ultrasound transceiver and the Medipix2 triple detector with multiple pinhole collimators on opposite halves of the cylindrical probe sharing the same central planar physical support and both will be aligned to the implantation template grid with a common spatial coordinate frame. A fixed thin ultrasound and radiation transparent cylindrical shell will be used to be in contact with the rectal wall while the built in linear array of the US transducer and the gamma camera of the probe will be rotated inside the shell acquiring US image of prostate and seeds radiation image without interfering with the rectum wall, minimizing the deformation of the volumes and the position of the organs during the treatment. BK Medical [27] in the recent past suggested the use of a linear array of the US transducer rotated inside of a thin cylindrical shell for radial 3D scanning, suggesting that the approach of Brachy*View* is feasible. This probe will provide co-registration of the seeds position in TRUS dataset automatically. The Brachy*View* probe may also be configured to allow simultaneous limited angle CT imaging of seeds for procedural post-implant dosimetry using a miniature X-ray tube rotated on an arc trajectory above the patient pelvis. CT imaging of active seeds can take advantage of a specific feature of Medipix2 that allows rejecting of events in specifically selected energy windows. For instance, selecting the energy window 22-36 keV, one should be able to reject all the background radiation from the implanted ^{125}I seeds and enhance CT contrast of the seeds image.

V. CONCLUSION AND FUTURE WORK

Studies using a high spatial resolution silicon detector for miniature in-body pinhole gamma camera have identified an opportunity for dynamic ITP in permanent implant prostate brachytherapy. A preliminary characterization of the Brachy*View* concept and reconstruction technique has been carried out by the use of a single Medipix2 sensor coupled to a single pinhole collimator. The seed position reconstruction method is based on triangulation of the image map of the seeds projected onto the imager surface through several pinholes. Proof of the feasibility of this approach was carried out using Model 6711 ^{125}I seeds placed at different locations in a PMMA phantom. The method demonstrates the feasibility of the 3D reconstruction of the seed center position with an accuracy better than 1mm for seeds located within 20 mm of the collimator. A model for estimating the 3D reconstruction accuracy based on the fundamental parameters of the camera has been implemented and validated by measurements. Further developments of the Brachy*View* project will attempt to improve the quality of the pinhole collimator using tungsten laser etching technology, manufacturing of the triple-chip Medipix detector on a single substrate and to integrate the high spatial resolution gamma camera with a TRUS probe. Future work will also include the development of a reconstruction method based on the use of the pattern of seed to identify the orientation of the seeds and software development for the imaging of multiple seeds in a realistic clinical scenario. The use of imaging techniques from the nuclear imaging field such as a coded aperture pinhole collimator combined with the well known geometry of the distrib-

uted activity in a seed would simplify the reconstruction of around one hundred seeds typically implanted into a prostate for a realistic treatment plan. This new device could condense prostate permanent implant brachytherapy into a single procedure wherein volumetric study, intra-operative dynamic treatment planning and post-implant dosimetry are all performed by a single device.

VI. ACKNOWLEDGMENTS

The authors would like to thank the National Health and Medical Research Council for its support of the research and development of the Brachy*View* probe under award NHMRC Research Grant 573428 as well as MEDIPIX collaboration.

Address of the corresponding author: marcop@uow.edu.au

VII. REFERENCES

1. J. Ferlay, H.R. Shin, F. Bray, F. Forman, C. Mathers and D.M. Parkin *GLOBOCAN 2008 v1.2, Cancer Incidence and Mortality Worldwide: IARC CancerBase No.10*. Available at http://globocan.iarc.fr (Accessed Feb. 2011).

2. J.F. Williamson, "Brachytherapy technology and physics practice since 1950: a half-century of progress" Phys. Med. Biol. **51**, R303–R325 (2006).

3. M. Zerbib, M.J. Zelefsky, C.S. Higano, P.R. Carroll "Conventional treatments of localized prostate cancer" Urology, **72**, (Suppl. 6), S25–S35, (2008).

4. Y. Yu "Permanent prostate seed implant brachytherapy: Report of the American Association of Physicists in Medicine Task Group No. 64" (1999).

5. J. Willins, K. Wallner "CT based dosimetry for transperineal I-125 prostate brachytherapy" Int. J. Radiat. Oncol. Biol. Phys., **39**, 347-353, (1997)

6. J.E. Dawson, T. Wu, T. Roy, J.Y. Gu, H. Kim "Dose effects Technical note of seeds placement deviations from preplanned positions in ultrasound guided prostate implants" Radiother. Oncol. **32**, 268-270, (1994)

7. Y. Yu, F.M. Waterman, N. Suntharalingam, A. Schulsinger "Limitations of the minimum peripheral dose as a parameter for dose specification in permanent ^{125}I prostate implants" Int. J. Radiat. Oncol. Biol. Phys., **34**, No. 3, 717-725, (1996)

8. M.J. Zelefsky, Y. Yamada, G. Cohen, E.S. Venkatraman, A.Y. Fung, E. Furhang, D. Silvern, M. Zaider "Postimplantation dosimetric analysis of permanent transperineal prostate implantation: improved dose distributions with an intraoperative computer-optimized conformal planning technique" Int. J. Radiation Oncology Biol. Phys. **48** (2), 601-608, (2000).

9. K. Wallner, J. Roy, M. Zelefsky, Z. Fuks, and L. Harrison. "Fluoroscopic visualization of the prostatic urethra to guide transperineal prostate implantation" Int. J. Radiation Oncology Biol. Phys. **29**, 863-867, (1994).

10. K. Wallner, S.T. Chiu-Tsao, J. Roy "An improved method for computerized tomography-planned transperineal 125-iodine prostate implants" J. Urol. **146**, 90-95, (1991).

11. J.N. Roy, K. Wallner, S. Chiu-Tsao "CT-based optimized planning for transperineal prostate implant with customized template" Int. J. Radiation Oncology Biol. Phys. **21**, 483-489, (1991).

12. M. J. Zelefsky, M. Worman, G.N. Cohen, X. Pei, M. Kollmeier, J. Yamada, B. Cox, Z. Zhang, E. Bieniek, L. Dauer "Real-time Intraoperative Computed Tomography Assessment of Quality of Permanent Interstitial Seed Implantation for Prostate Cancer" Urology **76**, Iss. 5, 1138-1142, (2010).

13. M.J. Zelefsky, Y. Yamada, G. Cohen, E.S. Venkatraman, A.Y.C. Fung, E. Furhang, D. Silvern, and M. Zaider "Postimplantation dosimetric analysis of permanent transperineal prostate implantation: improved dose distributions with an intraoperative computer-optimized conformal planning technique" Int. J. Radiation Oncology Biol. Phys. **48** (2), 601-608, (2000).

14. B.H. Han, K. Wallner, G. Merrick, W. Butler, S. Sutlief, and J. Sylvester "Prostate brachytherapy seed identification on post-implant trus images" Med. Phys. **30** (5), 898-900, (2003).

15. A. Polo, C. Salembier, J. Venselaar, P. Hoskin "Review of intraoperative imaging and planning techniques in permanent seed prostate brachytherapy" Radiother. Oncol. **94** (1), 12-23, (2010).

16. J.S. Eshleman, B.J. Davis, T. M. Pisansky, T.M. Wilson, M.G. Haddock, B.F. King, C.H. Darby, W.N. Lajoie, A.L. Oberg, "Radioactive Seed Migration to the Chest After Transperineal Interstitial Prostate Brachytherapy: Extraprostatic Seed Placement Correlates with Migration" Int. J. Radiation Oncology Biol. Phys. **59**, 2, 419-425, (2004).

17. A.W. Lehren and K. Rebelo "At V.A. Hospital, a Rogue Cancer Unit" New York Times, New York, (2009).

18. IAEA "Lessons learned from accidental exposure in radiotherapy" Report n.**17**, (2000).

19. J. Dammera, P.M. Frallicciardi, J. Jakubek, M. Jakubek, S. Pospisil, E. Prenerova, D. Vavrik, L. Volter, F. Weyda, R. Zemek "Real-time in-vivo m-imaging with Medipix2" Nucl. Instr. and Meth. A **607**, 205-207, (2009).

20. M. Fiederle "USB Lite – Miniaturized readout interface for Medipix2 detector" Nucl. Instrum. And Meth. A **592**, 121-125, (2010).

21. F.J. Beekman, D.P. McElroy, F. Berger, S.S. Gambhir, E.J. Hoffman "Towards in vivo nuclear microscopy: iodine-125 imaging" Eur. J. Nucl. Med. Molecol. Imag. **29**, 7 (2002).

22. E.N. Marieb, K. Hoehn "Human anatomy and physiology" Pearson International Edition (2004).

23. ONCURA "ONCOSEED - Model 6711 Specification sheet" Oncura, Arlington Heights, IL 60004 USA, (2009).

24. D.J. Brady, L. Marks "Three-dimensional source reconstruction with a scanned pinhole camera" Optics Letters **23**, No.11 (1998).

25. F. Beekman "The pinhole: gateway to ultra-high-resolution three-dimensional radionuclide imaging" Eur. J. Nucl. Med. Molecol. Imag. **34**, 2 (2007).

26. S. Koprulu, I. Cevik, N. Unlu, O. Dillioglugil "Size of the transrectal ultrasound probe makes no difference in pain perception during TRUS-Bx under adequate local anesthesia" Int. Urol. Nephrol. **44**, 1, 29-33, (2012).

27. BK MEDICAL - http://www.bkmed.com/3dart_transducer_8838_en.htm (Accessed September 2012).

Figure caption list

Fig. 1: Schematic of Brachy*View* rectal probe. Three side –by –side Medipix detectors are placed inside of the TRUS probe and inferiorly to the prostate gland.

Fig.2: a) Model of the pinhole used for the design of the collimator/camera setting; b)Scanning Electron Microscope of the pinhole for evaluation of the real dimensions of the aperture used during the experiments.

Fig.3: Schematic of the prostate phantom setup for seed image acquisition based on a single Medipix. The pitch of the holes housing the seeds is 10 mm. The distance between the sensor surface and the collimator 5.5 mm and the minimum distance of a seed from the collimator is approximately 10 mm. The prostate phantom is a block of PMMA of 6x6x6 cm^3

Fig.4: Schematic representation of the homogeneous coordinate model and reconstruction method by triangulation. The left side figure represents the first projection of the seeds: seed D3 is blocked by seed B3 and in the image plane only three seeds are visible. In the right side figure, the grey image plane represents the first projection; after a translation step backward to *Y* direction of the probe, all 4 seeds are visible on the image plane.

Fig.5: a) Response map of Brachy*View* to 4 seeds placed into positions B1, C2, B3, A4 of the phantom; b) response profile at column *Y*=120 and fit by Gaussian distribution for calculation of the spatial resolution FWHM; c) comparison of FWHM values obtained from the response map of the Brachy*View* camera (solid squares) and transverse accuracy in the plane *XY* (solid triangles) for different *Z* positions of seeds and predicted by the model from Beekman[24] and from Marks [25].

Fig.6. a) Medipix response maps of 5 implanted seeds at positions A2, A4, B1, B3, B5. The shape of each seed is clearly visible. Note that in the third image at the top, the seeds in positions B1 and B5 are blocked from view by seeds in row A. Each view is taken at 5mm increments along the *Y*-axis. b) schematic representation of the seeds inside the phantom.

Fig.7: Medipix response map of 5 seeds implanted at positions E1, E2, E3, E4 and E5. The shape of each seed is not visible anymore but the centre of mass can be still resolved and used for 3D reconstruction of the seed position.

Fig.8: Comparison of the reconstructed and expected seed positions in a phantom based on the centre-of-mass of the seeds in the *XZ* plane; *Y* is kept constant.